A Prokaryotic Voltage-Gated Sodium Channel

Dejian Ren,[1]* Betsy Navarro,[1,2]* Haoxing Xu,[1]* Lixia Yue,[1]* Qing Shi,[1] David E. Clapham[1]†

The pore-forming subunits of canonical voltage-gated sodium and calcium channels are encoded by four repeated domains of six-transmembrane (6TM) segments. We expressed and characterized a bacterial ion channel (NaChBac) from *Bacillus halodurans* that is encoded by one 6TM segment. The sequence, especially in the pore region, is similar to that of voltage-gated calcium channels. The expressed channel was activated by voltage and was blocked by calcium channel blockers. However, the channel was selective for sodium. The identification of NaChBac as a functionally expressed bacterial voltage-sensitive ion-selective channel provides insight into both voltage-dependent activation and divalent cation selectivity.

Voltage-gated potassium (K_v), sodium (Na_v), and calcium (Ca_v) channels underpin specialized higher order cell functions such as excitability, contraction, secretion, and synaptic transmission (*1*). Hundreds of K_v, Na_v, and Ca_v channel proteins provide the tremendous functional diversity required for the complex behaviors of eukaryotic vertebrate and invertebrate cell types (*2, 3*). Ion channels are also widespread in prokaryotes, but their gating and function are poorly understood because few have been functionally expressed in a system in which their properties can be studied.

The primary structural characteristic of ion-selective channels is a pore region surrounded by two-transmembrane (2TM) segments. The first high-resolution images of a bacterial 2TM tetrameric channel revealed the structural basis of K^+ ion selectivity encoded by the signature Gly-Tyr-Gly or Gly-Phe-Gly amino acid sequence in the pore region (*4*). In the primary structure of voltage-sensitive ion channels, an additional four transmembrane segments precede the pore-containing domain. The pore-forming subunits (α_1) of Na_v and Ca_v are composed of four similar repeats of 6TM domains (*3, 5*). It is thought that gene duplication of the 6TM K_v or TRP channels might have provided the precise structural requirements for highly selective Na^+ and Ca^{2+} channels. In particular, selectivity for Ca^{2+} requires coordination of the Ca^{2+} ions by four negatively charged glutamic or aspartic acid residues lining the pore. Members of the TRP class of ion channels are presumably tetramers of single 6TM subunits, but only a subset of these channels are moderately Ca^{2+}-selective (*6*). Here we report that a bacterial channel with strong similarity to the pore domains of Ca_v (*7*) is a voltage-dependent Na^+-selective channel. The properties of this presumably tetrameric channel closely mimic those of Na_v.

We previously isolated a mammalian putative voltage-gated cation channel, CatSper (*8*). CatSper is unique in that its amino acid sequence, especially in the putative pore region, is similar to that of Ca_v, even though CatSper is a 6TM protein. CatSper is required for cyclic nucleotide-mediated Ca^{2+} signaling in sperm and is essential for male fertility. Expression of CatSper in heterologous systems did not yield a detectable current. In a search for CatSper homologs for functional analysis, we discovered a putative gene assembled by shotgun sequencing of *B. halodurans* [(*9*), GenBank accession number BAB05220].

Isolation and sequencing of the gene encoding NaChBac (*10*) revealed an open reading frame (ORF) of 274 amino acids with a predicted molecular size of 31 kD and a calculated isoelectric point of 9.35 (Fig. 1A). NaChBac expressed in bacteria migrated during SDS–polyacrylamide gel

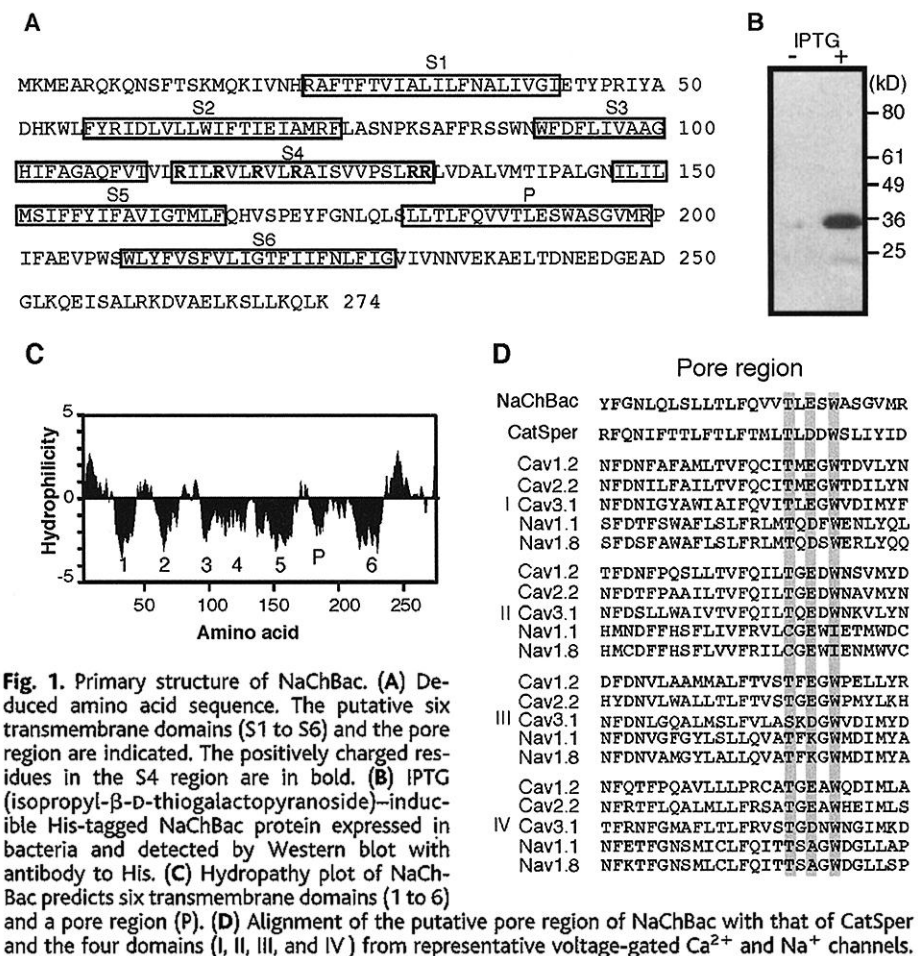

Fig. 1. Primary structure of NaChBac. **(A)** Deduced amino acid sequence. The putative six transmembrane domains (S1 to S6) and the pore region are indicated. The positively charged residues in the S4 region are in bold. **(B)** IPTG (isopropyl-β-D-thiogalactopyranoside)–inducible His-tagged NaChBac protein expressed in bacteria and detected by Western blot with antibody to His. **(C)** Hydropathy plot of NaChBac predicts six transmembrane domains (1 to 6) and a pore region (P). **(D)** Alignment of the putative pore region of NaChBac with that of CatSper and the four domains (I, II, III, and IV) from representative voltage-gated Ca^{2+} and Na^+ channels. GenBank accession numbers for sequences used in the alignment are AF407332 (CatSper), X15539 ($Ca_v1.2$), M94172 ($Ca_v2.2$), 054898 ($Ca_v3.1$), X03638 ($Na_v1.1$), and X92184 ($Na_v1.8$). Single-letter abbreviations for amino acid residues are as follows: A, Ala; C, Cys; D, Asp; E, Glu; F, Phe; G, Gly; H, His; I, Ile; K, Lys; L, Leu; M, Met; N, Asn; P, Pro; Q, Gln; R, Arg; S, Ser; T, Thr; V, Val; W, Trp; and Y, Tyr.

[1]Howard Hughes Medical Institute, Children's Hospital, Harvard Medical School, Enders 1309, 320 Longwood Avenue, Boston, MA 02115, USA. [2]Centro Internacional de Fisica, lab. de Biofisica, Bogota, Colombia.

*These authors contributed equally to this work.
†To whom correspondence should be addressed. E-mail: dclapham@enders.tch.harvard.edu

electrophoresis with an apparent molecular mass of ~34 kD (Fig. 1B). Hydrophobicity analysis was consistent with a primary structure containing 6TM domains (Fig. 1C). NaChBac contains an S4 segment characteristic of voltage-gated ion channels, with positively charged amino acids (Lys or Arg) interspersed every third residue (Fig. 1A). A BLAST search against the database revealed that the functional proteins with the closest similarity to NaChBac are Ca_v channels (7). In contrast to Ca_v channels that have four negatively charged amino acids in the pore, Na_v channels have glutamate or aspartate residues in domains

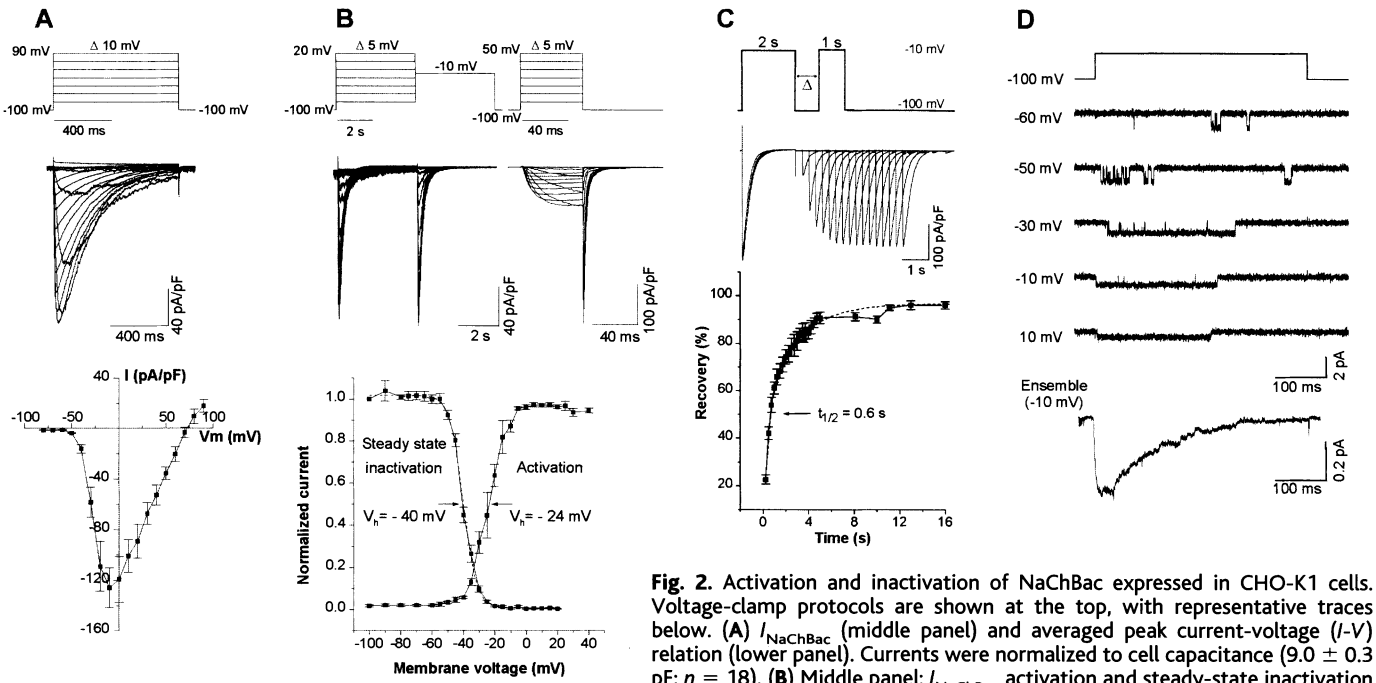

Fig. 2. Activation and inactivation of NaChBac expressed in CHO-K1 cells. Voltage-clamp protocols are shown at the top, with representative traces below. (**A**) $I_{NaChBac}$ (middle panel) and averaged peak current-voltage (*I-V*) relation (lower panel). Currents were normalized to cell capacitance (9.0 ± 0.3 pF; n = 18). (**B**) Middle panel: $I_{NaChBac}$ activation and steady-state inactivation currents. Lower panel: normalized activation curve (n = 21, ±SEM) and steady-state inactivation curve (n = 19, ±SEM). (**C**) Recovery from inactivation. The time interval between the test pulse (−10 mV, 2000 ms) and the inactivation pulse (−10 mV, 1000 ms) was varied from 250 ms to 16 s. The ratios between currents elicited by the two pulses were used to construct the recovery curve (n = 20, ±SEM). The half-time for recovery was 660 ms. (**D**) $I_{NaChBac}$ single channels and ensemble average.

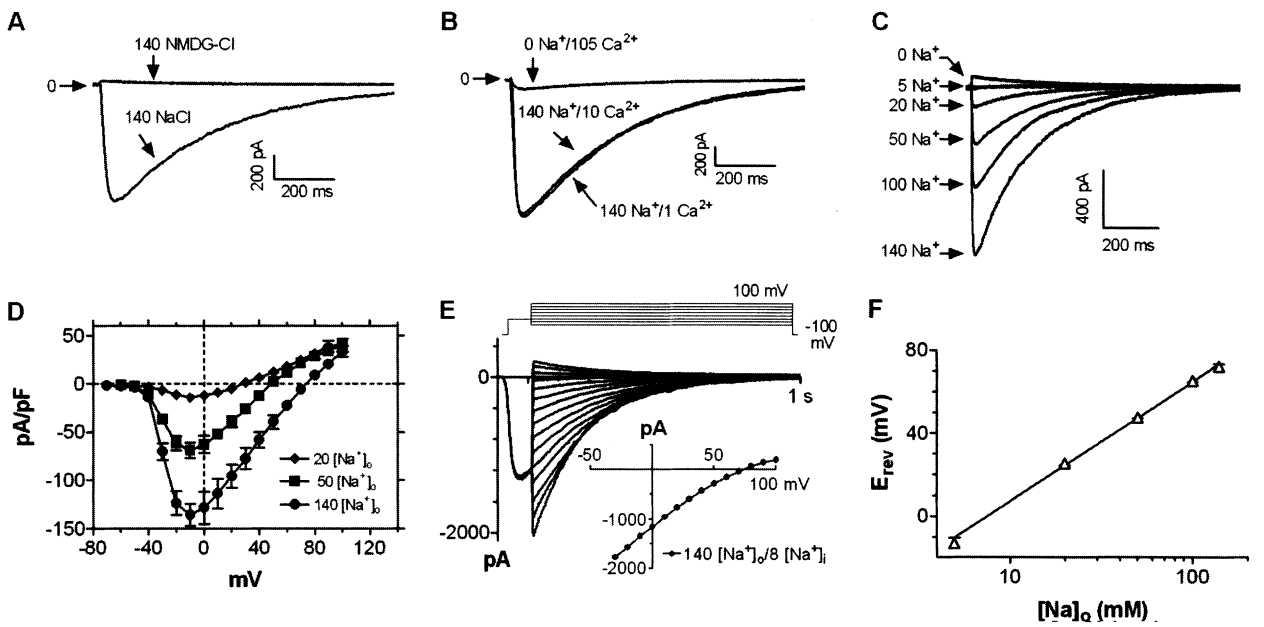

Fig. 3. Ion selectivity of $I_{NaChBac}$. (**A**) Impermeability of $I_{NaChBac}$ to Cl^- as shown by cation substitution with NMDG. (**B**) Low permeability of $I_{NaChBac}$ to Ca^{2+}. Peak current in isotonic $[Ca^{2+}]_o$ was 87 pA (7.6 ± 0.9 pA/pF, n = 8) compared to 1430 pA (135.9 ± 11 pA/pF, n = 8) in 140 mM $[Na^+]_o$/1 mM $[Ca^{2+}]_o$. (**C**) $I_{NaChBac}$ conductances at various values of $[Na^+]_o$. Current traces in (A) to (C) were elicited by a test pulse to −10 mV; holding potential V_H = −100 mV. (**D**) Mean current density plotted as a function of test potential in the presence of 20, 50, and 140 mM $[Na^+]_o$ (n = 8, ±SEM). (**E**) Tail currents recorded at various test potentials after depolarizing to 0 mV. $I_{NaChBac}$ tail current amplitudes plotted as a function of test potential were used to determine reversal potentials (inset). $[Ca^{2+}]_o \approx 10$ μM; capacitance = 9.1, 8.6, and 9.7 pF for (A), (C), and (E), respectively. (**F**) E_{rev} as a function of $[Na^+]_o$. The $E_{rev}/[Na^+]_o$ relation was best fit by a line with slope of 57.8 mV/decade (error bars are smaller than symbols).

I and II but lysine and alanine in domains III and IV (Fig. 1C). Replacing the lysine and alanine in domains III and IV of Na_v with glutamic acid conferred Ca^{2+} channel properties on the Na_v channel (*11*). A functional Ca_v or Na_v composed of only six transmembrane domains has never been effected, despite several attempts to artificially divide the large four-repeat α_1 subunits into single repeats (*12, 13*).

We examined whether NaChBac could yield a functional channel current in a heterologous expression system. We transfected NaChBac into CHO-K1 (Chinese hamster ovary) or COS-7 (green monkey kidney) cell lines and recorded whole-cell current 24 to 48 hours after transfection (*14*). NaChBac-transfected cells displayed large (~1000 to >10,000 pA) voltage-activated inward currents (Fig. 2A). This large current is unlike the small (50 pA), fast-inactivating, tetrodotoxin (TTX)-sensitive current (*15*) present in up to 20% of native CHO cells. Similar currents were not recorded in nontransfected or mock-transfected CHO-K1 or COS-7 cells. NaChBac-mediated current ($I_{NaChBac}$) reversed at +70 mV, close to the Nernst potential of Na^+ (E_{Na} = +72 mV). The activation of $I_{NaChBac}$ (τ_{act} = 12.9 ± 0.4 ms at –10 mV, n = 32) was slow relative to currents conducted by Na_v channels (τ_{act} < 2 ms). Inactivation was also slow (τ_{inact} = 166 ± 13 ms at –10 mV, n = 32) relative to the typically fast-inactivating Na_v current [τ_{inact} < 10 ms (*1*)].

We evaluated voltage-dependent activation by measuring the deactivation tail current (Fig. 2B). A Boltzmann fit of the averaged activation curve yielded a midpoint voltage V_h of –24 mV. Steady-state inactivation of the channel was determined by sequential depolarization to test voltages followed by clamp to the peak of activation at –10 mV. Steady-state inactivation was a steep function of voltage, with 50% inactivation at –40 mV (Fig. 2B). The channel recovered slowly from inactivation (Fig. 2C), with 50% recovery by 660 ms and 90% recovery by 5.5 s (–100 mV).

The single-channel properties of NaChBac were studied in the inside-out patch configuration (*16*). The unitary single-channel conductance was best fit with a slope of 12 ± 1 pS (n = 7 cells). Consistent with the whole-cell current, single channels were activated by depolarization, and both open and closed times varied as a function of voltage (*17*). An ensemble average of single-channel currents from five cells resembled whole-cell $I_{NaChBac}$, with τ_{act} = 10 ± 3.5 ms and τ_{inact} = 203 ± 43 ms (Fig. 2D).

Cation replacement with *N*-methyl-D-glutamine (NMDG) resulted in the complete removal of voltage-dependent inward current (Fig. 3A), which suggested that NaChBac was impermeant to anions (*18*). $I_{NaChBac}$ was weakly permeant to Ca^{2+}; no significant difference in current was observed by sequential perfusion with bath solution containing 1 and 10 mM extracellular calcium ($[Ca^{2+}]_o$) (Fig. 3B). In isotonic $[Ca^{2+}]_o$ (cations replaced with 105 mM Ca^{2+}), the inward current was <6% of that in normal $[Na^+]_o$ (140 mM extracellular Na^+) (7.6 ± 0.9 pA/pF at –10 mV, n = 8; Fig. 3B). In contrast, $I_{NaChBac}$ amplitude correlated well with $[Na^+]_o$ (Fig. 3, C and D). To estimate the reversal potential (E_{rev}) of $I_{NaChBac}$, we measured deactivation tail currents (Fig. 3E). Measured reversal potentials plotted as a function of $[Na^+]_o$ had a slope of 57.8 mV per decade, close to the slope predicted for a Na^+-selective pore (58 mV per decade). To estimate the relative ion selectivity of the channel, we measured changes in reversal potential while changing ionic composition. The calculated relative selectivity (±SEM) of NaChBac, as judged by measured E_{rev}, was P_{Na}/P_{Ca} = 72 ± 10 (n = 12); P_{Na}/P_{Cs} = 383 ± 56 (n = 8); P_{Na}/P_K = 171 ± 16 (n = 8). $I_{NaChBac}$ selectivity for Na^+ is at least as high as that of traditional Na_v channels (*1, 19*).

The pharmacological sensitivity of $I_{NaChBac}$ to Na_v and Ca_v blockers most closely resembled that of L-type Ca_v channels. Cd^{2+} (100 μM; Fig. 4A), Co^{2+} (1 mM), and La^{3+} (1 mM) all reduced the channel current to various degrees (Fig. 4F). $I_{NaChBac}$ was most sensitive to two dihydropyridines, nifedipine and nimodipine (Fig. 4, C, D, and G), with half inhibitory concentrations (IC_{50}s) of 2.2 μM and 1 μM, respec-

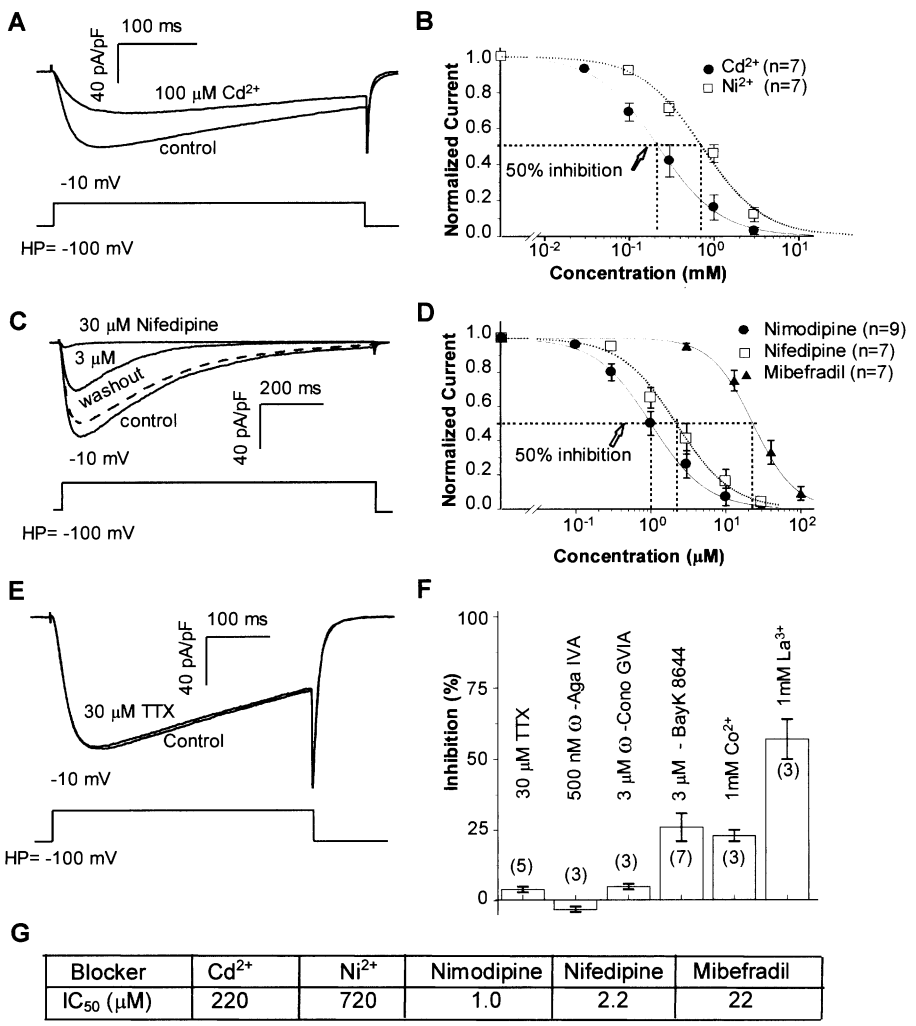

G

Blocker	Cd^{2+}	Ni^{2+}	Nimodipine	Nifedipine	Mibefradil
IC_{50} (μM)	220	720	1.0	2.2	22

Fig. 4. Sensitivity of $I_{NaChBac}$ to Ca_v and Na_v channel blockers. **(A)** Representative traces before (control) and after the addition of 100 μM Cd^{2+}. **(B)** $I_{NaChBac}$ dose-response curves to Cd^{2+} and Ni^{2+}. **(C)** $I_{NaChBac}$ was reversibly blocked by nifedipine. **(D)** $I_{NaChBac}$ sensitivity to the dihydropyridine class (nifedipine and nimodipine) of L-type Ca_v channel blockers and insensitivity to the T-type Ca_v channel blocker mibefradil. **(E)** Insensitivity of $I_{NaChBac}$ to TTX. **(F)** Summary of $I_{NaChBac}$ inhibition by various Ca_v-blocking agents. **(G)** Summary of concentration of agent needed to block $I_{NaChBac}$ by 50% (IC_{50}) as measured from dose-response curves.

tively (Fig. 4G). The dose-response curves for dihydropyridines are comparable to those for mammalian Ca_vs (*20*). $I_{NaChBac}$ was relatively insensitive to the T-type Ca_v channel antagonists mibefradil (IC_{50} = 22 μM) and Ni^{2+} (IC_{50} = 720 μM) (Fig. 4, B, D, and G). The Ca_v N-type blocker ω-conotoxin GVIA and the Ca_v P/Q blocker ω-agatoxin IVA were ineffective even at concentrations (3 μM and 500 nM, respectively) well above those used to block their respective targets (Fig. 4F). The channel was completely insensitive to the Na^+ channel blocker TTX (up to 30 μM; Fig. 4, E and F). The sensitivity of $I_{NaChBac}$ to dihydropyridines is not obvious from a sequence comparison to the known sites for Ca_v dihydropyridine sensitivity (*21–23*). Not surprisingly, the residues involved in Na_v TTX binding (*24–27*) do not match identically to residues in NaChBac.

NaChBac encodes a 6TM domain, dihydropyridine-sensitive, TTX-insensitive Na^+-selective current. $I_{NaChBac}$ differs from traditional 24TM Na_v eukaryotic channels in its slower (roughly one-tenth the speed of Na_v) activation, inactivation, and recovery from inactivation. The slow inactivation kinetics are similar to those of mammalian persistent sodium current I_{NaP} (*28*). A noninactivating, TTX-insensitive voltage-gated Na^+ channel current has been recorded from mammalian dorsal root ganglion neurons, but its sensitivity to dihydropyridines is not known (*29*). NaChBac-related mammalian homologs may account for some persistent Na^+ currents.

We can make several conclusions from the ability of NaChBac to form functional voltage-gated Na^+ selective channels. First, Na^+ selectivity does not require the four-domain repeat structure present in Na_v channels. Proper orientation of the selectivity filter can presumably be made in homotetramers of NaChBac. Second, the presence of glutamic and aspartic residues in the pore does not ensure Ca^{2+} selectivity. Third, as is apparent from the defined Ca_v and Na_v sites for dihydropyridine and TTX block, pharmacologic sensitivity need not be correlated with channel selectivity.

NaChBac should facilitate studies of the activation and inactivation gates of the sodium channel. Recently, Hilber *et al.* (*30*) showed that when the domain IV 1529 alanine residue of rat skeletal muscle Na_v was substituted by aspartic acid, inactivation was drastically slowed and recovery time constants were slowed to the 100-s range, implying that the selectivity filter is involved in channel gating. Interestingly, the corresponding residue in the slowly inactivating NaChBac is a glutamic acid.

Hypothetically, Ca_v channels may require a flexible tertiary structure around the glutamate and aspartate residues in the pore to enable the channel filter to bind one Ca^{2+} ion with high affinity or two with lower affinity (*31*). This Ca^{2+} binding flexibility may be provided by the similar but nonidentical amino acids surrounding the glutamate and aspartate residues in the four repeats in the pore-forming α_1 subunit (*32*). Because all four repeats are presumably identical in a NaChBac tetramer, this flexibility is lost. Heterotetramers of NaChBac homologs might recreate this flexible environment to allow formation of Ca^{2+}-selective channels, considerably increasing the diversity of this channel class. The simple NaChBac channel thus emphasizes the evolutionary utility of the 6TM building block.

We have not tested the biological role of NaChBac in the extremophile *B. halodurans*. This bacterium lives in extremely high salt (up to 1 M), highly alkaline (up to pH 11) conditions, and thus Na^+ influx through the open channel should be large. Na^+ drives the flagellar motor used by alkaphilic *Bacillus* (*33–36*), and NaChBac is a good candidate for control of flagellar activity. Regardless of its prokaryotic function, NaChBac's signal importance will be in providing the protein needed for structural studies of the Na^+ selectivity filter and voltage sensor.

References and Notes

1. B. Hille, *Ion Channels of Excitable Membranes* (Sinauer, Sunderland, MA, ed. 3, 2001).
2. C. M. Armstrong, B. Hille, *Neuron* **20**, 371 (1998).
3. W. A. Catterall, *Neuron* **26**, 13 (2000).
4. D. A. Doyle *et al.*, *Science* **280**, 69 (1998).
5. C. Sato *et al.*, *Nature* **409**, 1047 (2001).
6. D. E. Clapham, L. W. Runnels, C. Strubing, *Nature Rev. Neurosci.* **2**, 387 (2001).
7. S. R. Durell, H. R. Guy, *Biochem. Biophys. Res. Commun.* **281**, 741 (2001).
8. D. Ren *et al.*, *Nature* **413**, 603 (2001).
9. H. Takami *et al.*, *Nucleic Acids Res.* **28**, 4317 (2000).
10. NaChBac was cloned from *Bacillus halodurans* C-125 DNA by the polymerase chain reaction (PCR) using Pfu polymerase and primers designed according to the deposited sequence (GenBank accession number BAB05220). The deduced sequence is identical to the deposited sequence except for two differences: nucleotide 35 (T in our clone versus C in the deposited sequence; no change in amino acid) and nucleotide 818 (T versus C; Leu to Ser amino acid change). There is a large deletion (>1 kb) in the deposited sequence immediately after the ORF. Multiple clones from different amplification reactions were sequenced to verify our cDNA. Errors in the deposited C-125 sequence probably result from the shotgun method of sequence assembly.
11. S. H. Heinemann, H. Terlau, W. Stuhmer, K. Imoto, S. Numa, *Nature* **356**, 441 (1992).
12. W. Stuhmer *et al.*, *Nature* **339**, 597 (1989).
13. C. A. Ahern *et al.*, *Proc. Natl. Acad. Sci. U.S.A.* **98**, 6935 (2001).
14. NaChBac was subcloned into a pTracer-CMV2 vector (Invitrogen) containing enhanced green fluorescent protein (eGFP) for expression in CHO-K1 and COS-7 cells. DNA was transfected with LT2 polyamine transfection reagent (PanVera) and plated onto cover slips, and recordings were made 24 to 48 hours later. Unless otherwise stated, the pipette solution contained 147 mM Cs, 120 mM methanesulfonate, 8 mM NaCl, 10 mM EGTA, 2 mM Mg–adenosine triphosphate, and 20 mM Hepes (pH 7.4). Bath solution contained 130 mM NaCl, 10 mM $CaCl_2$, 5 mM KCl, 20 mM Hepes (pH 7.4), and 10 mM glucose. All experiments were conducted at 22° ± 2°C. Unless otherwise indicated, all chemicals were dissolved in water. Nifedipine (dissolved in dimethyl sulfoxide), ω-agatoxin IVA, ω-conotoxin GVIA, and (±)Bay K 8644 (dissolved in ethanol) were purchased from Alomone Labs. TTX, nimodipine (dissolved in methanol), and all metal ion blockers were from Sigma. When water was not the solvent, the final concentration of the solvents was less than 1% and did not affect the channel activity. Unknown agents, presumably leached from perfusion tubing, caused apparent fast inactivation, and these perfusion systems were subsequently avoided.
15. R. Skryma, N. Prevarskaya, P. Vacher, B. Dufy, *Am. J. Physiol.* **267**, C544 (1994).
16. Single-channel currents were recorded in the inside-out configuration. Solutions were the same as used in whole-cell recording except that the pipette and bath solutions were reversed.
17. B. Navarro *et al.*, unpublished data.
18. The internal pipette solution used in determining the relative permeability of K^+ and Ca^{2+} contained 133 mM Cs-methanesulfonate, 5 mM CsCl, 10 mM EGTA, and 10 mM Hepes (pH adjusted to 7.2 with CsOH). External solution for K^+ permeability experiments contained 142 mM KCl, 10 mM Hepes (pH 7.3, adjusted with KOH), and 10 mM glucose. External solution for Ca^+ permeability determinations contained 105 mM $CaCl_2$, 10 mM Hepes [pH 7.3, adjusted with $Ca(OH)_2$], and 20 mM glucose. The external solution used to study Na^+ permeability contained 140 mM NaCl, 5 mM CsCl, 10 mM Hepes (pH 7.3, adjusted with NaOH), and 10 mM glucose. Internal solutions were the same as described in (*14*). The relative permeability of Cs^+ versus Na^+ was calculated according to

$$P_{Cs}/P_{Na} = \{[Na]_o - [Na]_i \exp(E_{rev}F/RT)\}/\{[Cs]_i \exp(E_{rev}F/RT) - [Cs]_o\} \quad (1)$$

where F is the Faraday constant. The relative permeability of K^+ and Ca^{2+} to Cs^+ was calculated according to the following equations (*1*):

$$P_K/P_{Cs} = [Cs]_i \exp(E_{rev}F/RT)/[K]_o \quad (2)$$

$$P_{Ca}/P_{Cs} = [Cs]_i \exp(E_{rev}F/RT)\,[\exp(E_{rev}F/RT) + 1]/4[Ca]_o \quad (3)$$

19. Y. M. Sun, I. Favre, L. Schild, E. Moczydlowski, *J. Gen. Physiol.* **110**, 693 (1997).
20. D. J. Triggle, *Eur. J. Pharmacol.* **375**, 311 (1999).
21. G. H. Hockerman, B. Z. Peterson, B. D. Johnson, W. A. Catterall, *Annu. Rev. Pharmacol. Toxicol.* **37**, 361 (1997).
22. S. Yamaguchi, Y. Okamura, T. Nagao, S. Adachi-Akahane, *J. Biol. Chem.* **275**, 41504 (2000).
23. E. Wappl, J. Mitterdorfer, H. Glossmann, J. Striessnig, *J. Biol. Chem.* **276**, 12730 (2001).
24. H. Terlau *et al.*, *FEBS Lett.* **293**, 93 (1991).
25. P. H. Backx, D. T. Yue, J. H. Lawrence, E. Marban, G. F. Tomaselli, *Science* **257**, 248 (1992).
26. J. Satin *et al.*, *Science* **256**, 1202 (1992).
27. L. Sivilotti, K. Okuse, A. N. Akopian, S. Moss, J. N. Wood, *FEBS Lett.* **409**, 49 (1997).
28. W. E. Crill, *Annu. Rev. Physiol.* **58**, 349 (1996).
29. T. R. Cummins *et al.*, *J. Neurosci.* **19**, RC43 (1999).
30. K. Hilber *et al.*, *J. Biol. Chem.* **276**, 27831 (2001).
31. P. T. Ellinor, J. Yang, W. A. Sather, J. F. Zhang, R. W. Tsien, *Neuron* **15**, 1121 (1995).
32. J. Yang, P. T. Ellinor, W. A. Sather, J. F. Zhang, R. W. Tsien, *Nature* **366**, 158 (1993).
33. Y. Imae, T. Atsumi, *J. Bioenerg. Biomembr.* **21**, 705 (1989).
34. T. Atsumi, L. McCarter, Y. Imae, *Nature* **355**, 182 (1992).
35. T. A. Krulwich, M. Ito, A. A. Guffanti, *Biochim. Biophys. Acta* **1505**, 158 (2001).
36. T. Yorimitsu, M. Homma, *Biochim. Biophys. Acta* **1505**, 82 (2001).

37. We thank Y. Kirichock and T. Krulwich for helpful comments and A. Jackson for critical reading of the manuscript. Supported by the Howard Hughes Medical Institute.

22 August 2001; accepted 25 September 2001